SUPPLEMENTAL FIGURES

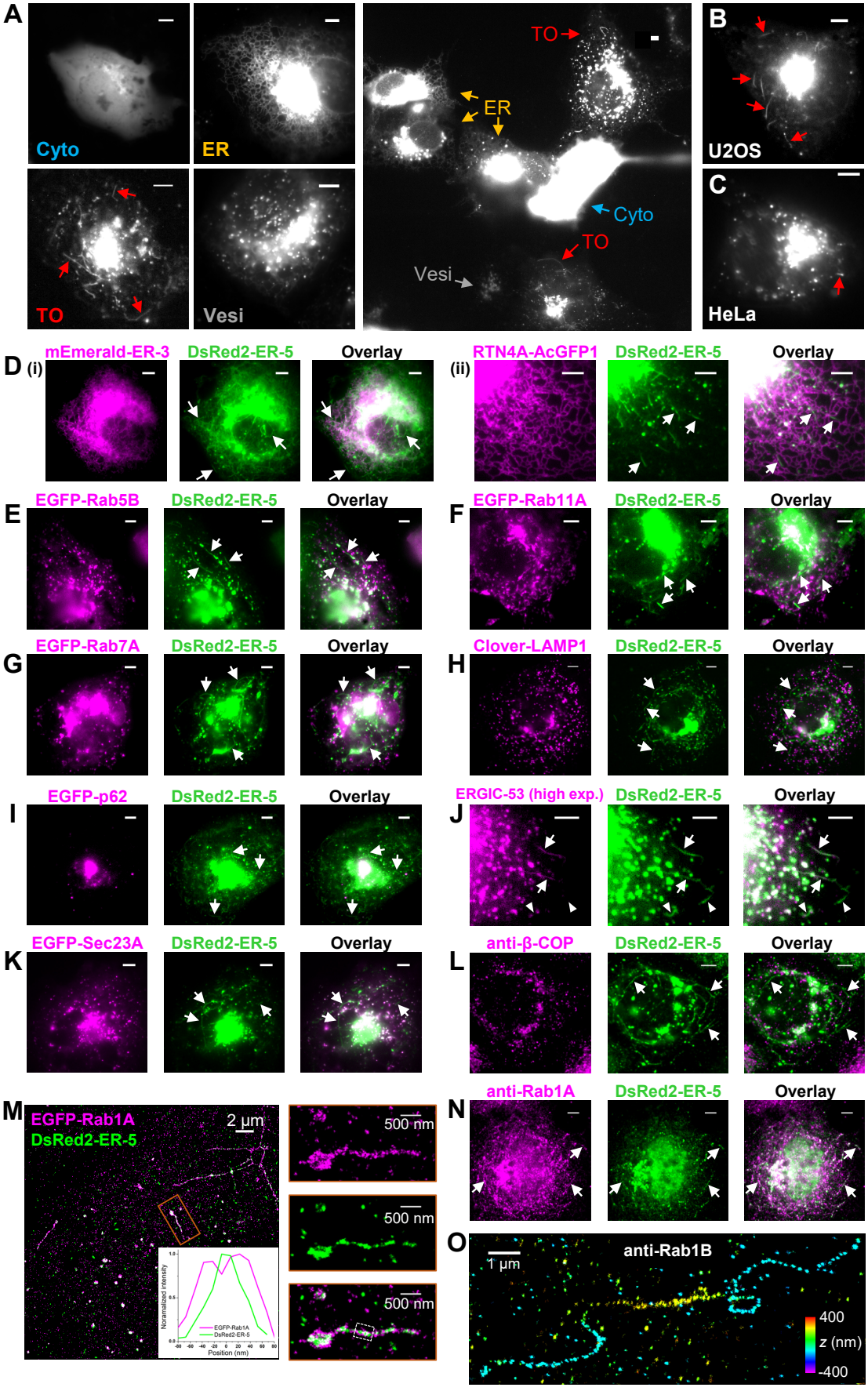

Figure S1. Characterization of DsRed2-ER-5-Containing Tubular Organelles, Related to Figure 1

(A) Representative images of the four types of subcellular distribution of DsRed2-ER-5 in COS-7 cells: cytoplasm (Cyto), ER, tubular organelles (TOs), and vesicles (Vesi).

(B,C) Representative images of DsRed2-ER-5 TOs in U2OS (B) and HeLa (C) cells.

(D-K) Two-color fluorescence micrographs of DsRed2-ER-5 (green) in live COS-7 cells with the ER markers mEmerald-ER-3 [D-(i)] or RTN4A-AcGFP1 [D-(ii)], the early endosome marker EGFP-Rab5B (E), the recycling endosome marker EGFP-Rab11A (F), the late endosome marker EGFP-Rab7A (G), the lysosome marker Clover-LAMP1 (H), the autophagosome marker EGFP-p62 (I), the highly expressed ERGIC marker mEmerald-ERGIC-53 (J), and the ERES marker EGFP-Sec23A (K). Arrowheads in (J) indicate TOs negative for ERGIC-53.

(L) Immunofluorescence of the COPI vesicle marker β-COP vs. DsRed2-ER-5.

(M) Two-color STORM of immunolabeled DsRed2-ER-5 and EGFP-Rab1A showing that Rab1A decorates the surface of the TO. Right panels: separated and merged color channels for a zoom-in of the orange box marked in the left panel. Inset: cross-sectional intensity profiles for the two color channels along a TO, for the region marked by the dotted box in the zoom-in image.

(N) Immunofluorescence of endogenous Rab1A in the COS-7 cell, showing good colocalization with the DsRed2-ER-5 TOs.

(O) Additional 3D-STORM image of immunostained endogenous Rab1B in the untransfected COS-7 cell, highlighting a long, twisted TO. Color encodes axial position.

Scale bars: 5 μm except for the labeled scale bars in (M,O). Arrows point to TOs.

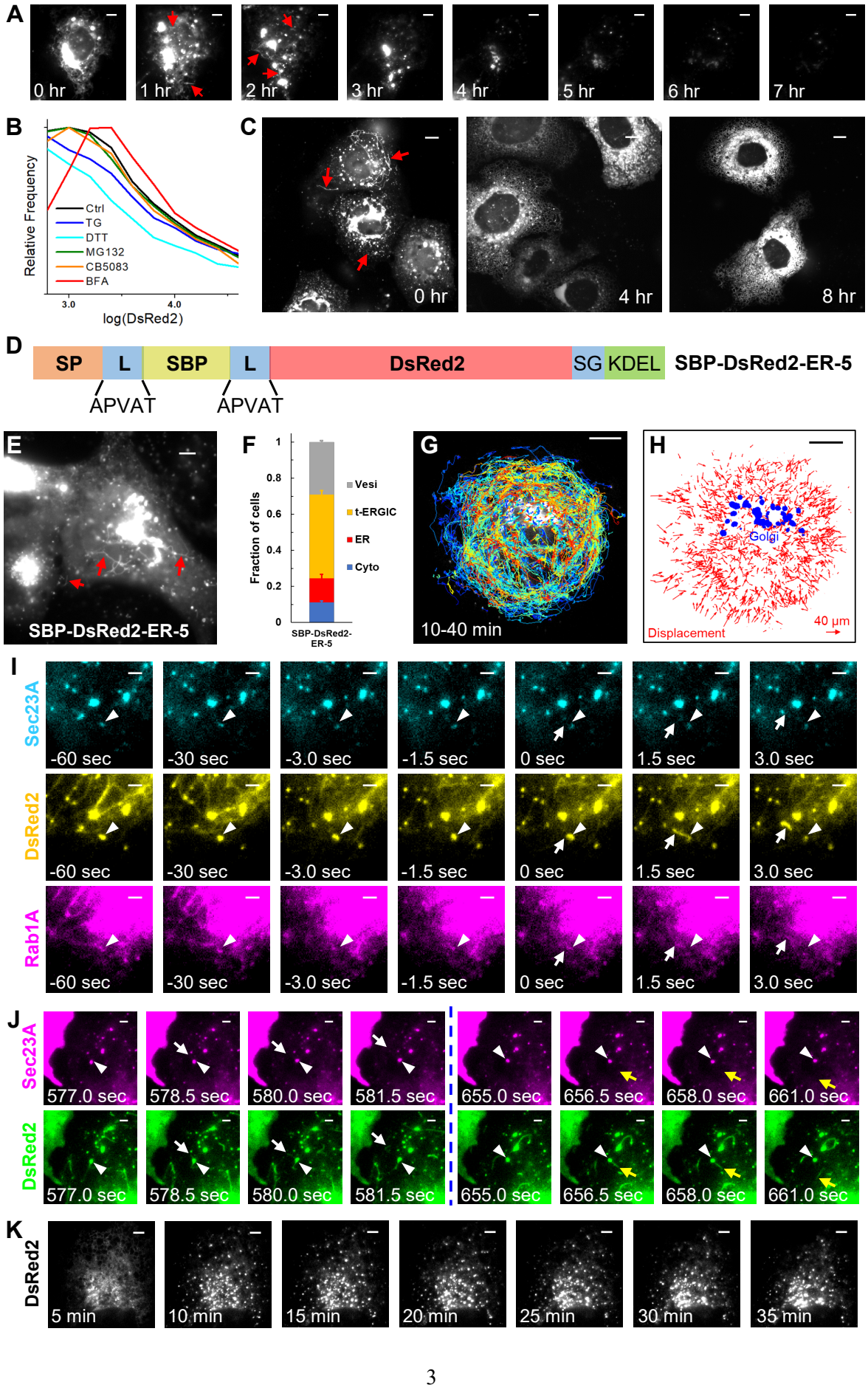
A
0 hr
1 hr
2 hr
3 hr
4 hr
5 hr
6 hr
7 hr
B
Relative Frequency
Ctrl
TG
DTT
MG132
CB5083
BFA
3.0
4.0
log(DsRed2)
C
0 hr
4 hr
8 hr
D
SP
L
SBP
L
DsRed2
SG KDEL
SBP-DsRed2-ER-5
APVAT
APVAT
E
SBP-DsRed2-ER-5
F
Fraction of cells
1
0.8
0.6
0.4
0.2
0
Vesi
t-ERGIC
ER
Cyto
SBP-DsRed2-ER-5
G
10-40 min
H
Golgi
40 μm
Displacement
I
Sec23A
DsRed2
Rab1A
-60 sec
-30 sec
-3.0 sec
-1.5 sec
0 sec
1.5 sec
3.0 sec
J
Sec23A
DsRed2
577.0 sec
578.5 sec
580.0 sec
581.5 sec
655.0 sec
656.5 sec
658.0 sec
661.0 sec
K
DsRed2
5 min
10 min
15 min
20 min
25 min
30 min
35 min

Figure S2. The t-ERGIC Mediates ER-to-Golgi Trafficking by Shuttling between the ER and the Golgi, Related to Figure 2

(A) Time-lapse imaging of DsRed2-ER-5 in an unsynchronized COS-7 cell, showing its redistribution from the ER to the TOs, Golgi, and vesicles accompanied by a reduction of fluorescence intensity.

(B) Flow cytometry histograms of DsRed2-ER-5-transfected COS-7 cells treated with 0.1% DMSO (Ctrl), 1 μM thapsigargin (TG), 7 mM dithiothreitol (DTT), 5 μM MG132, 1 μM CB-5083, or 1 μM brefeldin A (BFA) for 4 hr.

(C) Representative fluorescence micrographs of DsRed2-ER-5 in COS-7 cells with brefeldin A treatments of 0, 4, and 8 hr.

(D-F) Schematic of SBP-DsRed2-ER-5 (D), a representative image of its presence in the t-ERGIC (E), and its subcellular distribution (F) in transfected COS-7 cells. Error bars: SEM (n = 3 with ~50 cells in each replicate).

(G) Single-particle tracking of post-ER carriers in Figure 2D. The color of each trajectory encodes the maximum speed reached.

(H) Displacement map of the trajectories in (G). The Golgi apparatus is marked blue. Arrows point to the direction of displacement (from the initial position to the final position), and their magnitudes are scaled according to the legend.

(I) Another example of *de novo* formation of SBP-DsRed2-ER-5 t-ERGIC (arrow) from the ERES (arrowhead) in a RUSH experiment, similar to Figure 2G. 80 μM biotin was added at time -11 min for cargo release.

(J) RUSH image sequence showing that the same COPII-coated ERES (arrowhead) sequentially generates two t-ERGICs (white and yellow arrows) in opposite directions. 80 μM biotin was added at time 0.

(K) Co-transfection of SBP-DsRed2-ER-5 with a dominant negative Rab1A (Rab1A-N124I) inhibited the generation of t-ERGIC in RUSH, and the cargo was stuck at the ERES. 80 μM biotin was added at time 0.

Scale bars: 10 μm (C,G,H); 5 μm (A,E,K); 2 μm (I,J). Arrows in (A,C,E) indicate t-ERGICs.

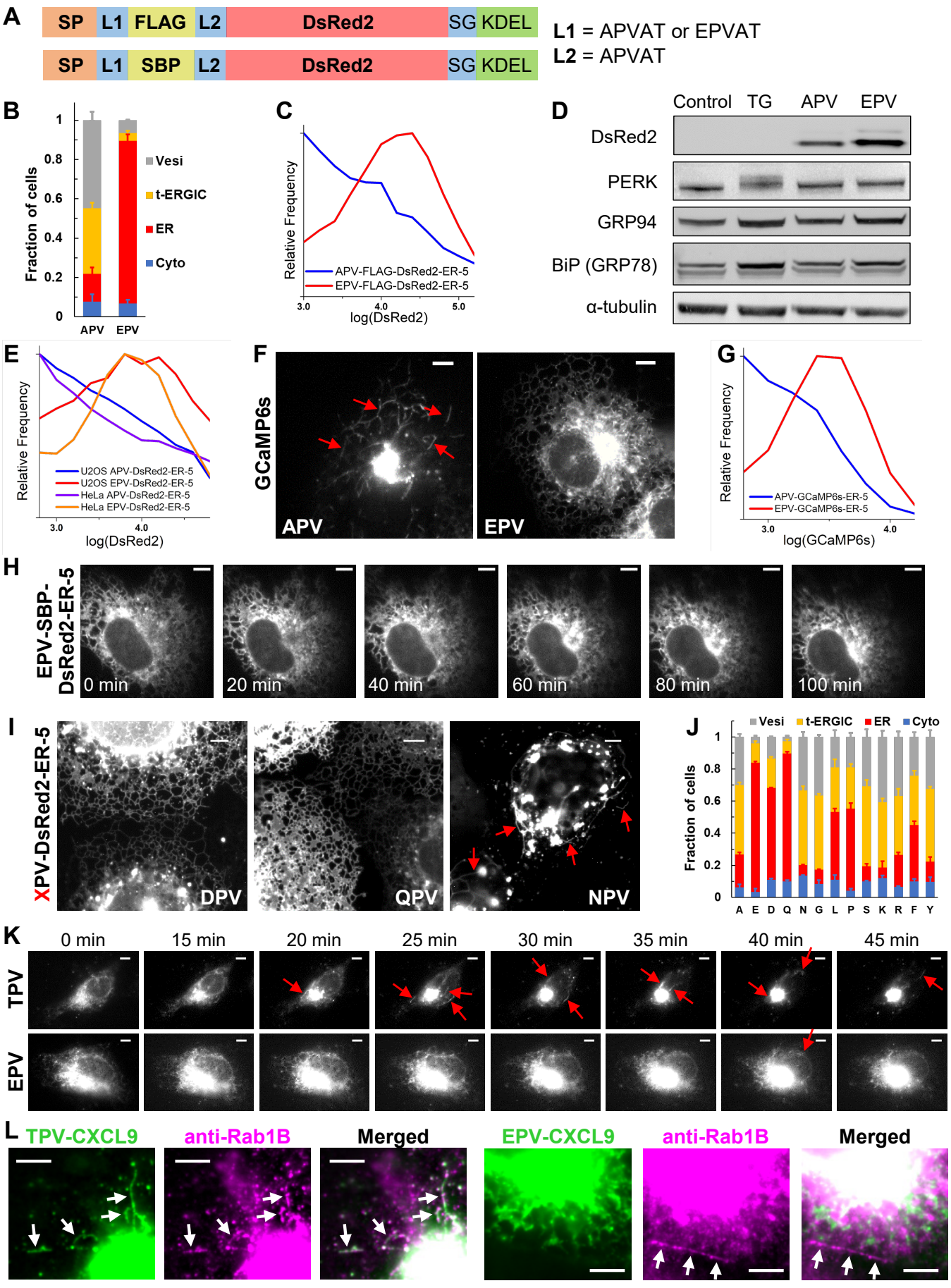
A
SP L1 FLAG L2 DsRed2 SG KDEL
SP L1 SBP L2 DsRed2 SG KDEL
L1 = APVAT or EPVAT
L2 = APVAT
B
Fraction of cells
Vesi
t-ERGIC
ER
Cyto
APV EPV
C
Relative Frequency
APV-FLAG-DsRed2-ER-5
EPV-FLAG-DsRed2-ER-5
log(DsRed2)
D
Control TG APV EPV
DsRed2
PERK
GRP94
BiP (GRP78)
α-tubulin
E
Relative Frequency
U2OS APV-DsRed2-ER-5
U2OS EPV-DsRed2-ER-5
HeLa APV-DsRed2-ER-5
HeLa EPV-DsRed2-ER-5
log(DsRed2)
F
GCaMP6s
APV
EPV
G
Relative Frequency
APV-GCaMP6s-ER-5
EPV-GCaMP6s-ER-5
log(GCaMP6s)
H
EPV-SBP-DsRed2-ER-5
0 min
20 min
40 min
60 min
80 min
100 min
I
XPV-DsRed2-ER-5
DPV
QPV
NPV
J
Vesi t-ERGIC ER Cyto
Fraction of cells
A E D Q N G L P S K R F Y
K
0 min 15 min 20 min 25 min 30 min 35 min 40 min 45 min
TPV
EPV
L
TPV-CXCL9
anti-Rab1B
Merged
EPV-CXCL9
anti-Rab1B
Merged

Figure S3. The N-terminus Rule of ER-to-Golgi Transport by t-ERGIC Applies to Different Cargoes, Related to Figure 3

(A) Sequences of APV/EPV-FLAG-DsRed2-ER-5 and APV/EPV-SBP-DsRed2-ER-5.

(B,C) Subcellular distributions (B) and flow cytometry histograms (C) of APV/EPV-FLAG-DsRed2-ER-5.

(D) Immunoblots of APV/EPV-DsRed2-ER-5-transfected cells and non-transfected cells with or without 1 μM thapsigargin (positive control for ER stress) treatment for 5 hr.

(E) Flow cytometry histograms of APV/EPV-DsRed2-ER-5 in HeLa and U2OS cells.

(F,G) Representative fluorescence micrographs (F) and flow cytometry histograms (G) of APV/EPV-GCaMP6s-ER-5 in COS-7 cells.

(H) Representative RUSH image sequence of EPV-SBP-DsRed2-ER-5. 80 μM biotin was added at time 0.

(I) Representative fluorescence micrographs of DPV/QPV/NPV-DsRed2-ER-5 in COS-7 cells.

(J) Subcellular distributions of different XPV-DsRed2-ER-5 variants. The “A” and “E” data duplicates that of “ER-5” in Figure 1D and that of Figure 3C, respectively.

(K) Representative RUSH image sequences of TPV/EPV-CXCL9-mCherry-SBP. Whereas the wild-type (TPV; top) exhibited efficient ER-to-Golgi transport via the t-ERGIC (arrow), the EPV mutant (bottom) was transported more slowly without appreciable t-ERGIC formation. 80 μM biotin was added at time 0. The “25 min” images correspond to Figure 3L.

(L) Representative two-color fluorescence micrographs of TPV/EPV-CXCL9-mCherry-SBP (green) and immunolabeled Rab1B (magenta) for RUSH experiments fixed at 25 min after biotin addition, showing substantial colocalization of the wild-type (TPV) version with the Rab1B-positive t-ERGIC tubules.

Scale bars: 5 μm. Error bars: SEM (n = 3 with ~50 cells in each replicate). Arrows point to t-ERGICs.

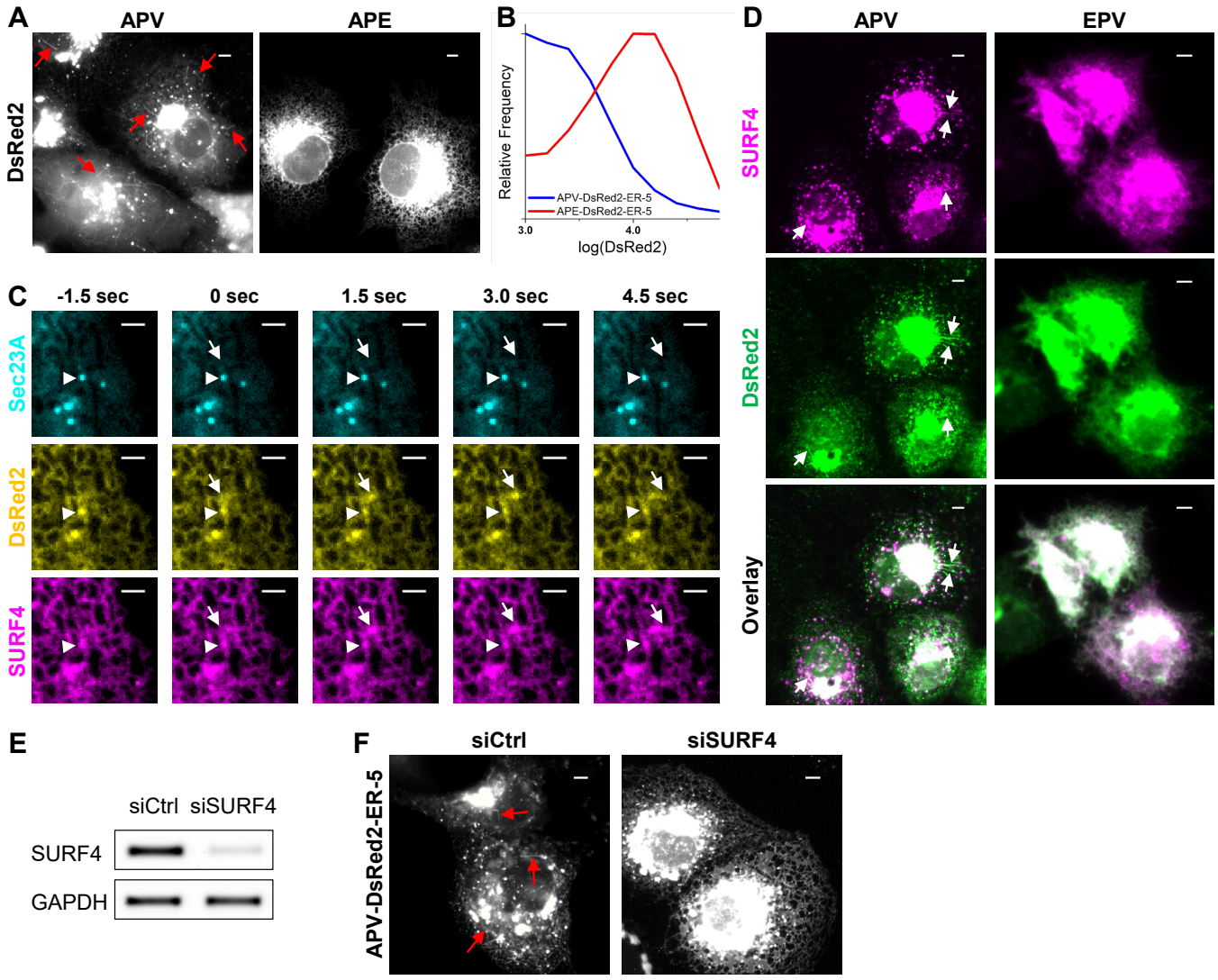

Figure S4. SURF4 Recognizes the N-terminus of the Cargo and Co-traffics with Its Selected Cargo via t-ERGICs, Related to Figure 4

(A,B) Representative fluorescence micrographs (A) and flow cytometry histograms (B) of APV/APE-DsRed2-ER-5 in COS-7 cells.

(C) Image sequence showing *de novo* generation of a t-ERGIC through the co-budding of AcGFP1-SURF4 (magenta) and APV-DsRed2-ER-5 (yellow) but not JF635-labeled HaloTag-Sec23A (cyan). Arrowhead marks the ERES. Arrow indicates the t-ERGIC.

(D) Representative immunofluorescence images of FLAG-SURF4 (magenta) in COS-7 cells co-transfected with APV/EPV-DsRed2-ER-5 (green).

(E) RT-PCR of SURF4 mRNA in control and SURF4 siRNA-treated cells.

(F) Representative live-cell images of APV-DsRed2-ER-5 in control and SURF4 siRNA-treated cells.

Arrows indicate t-ERGICs. Scale bars: 5 μm (A,D,F); 2 μm (C).

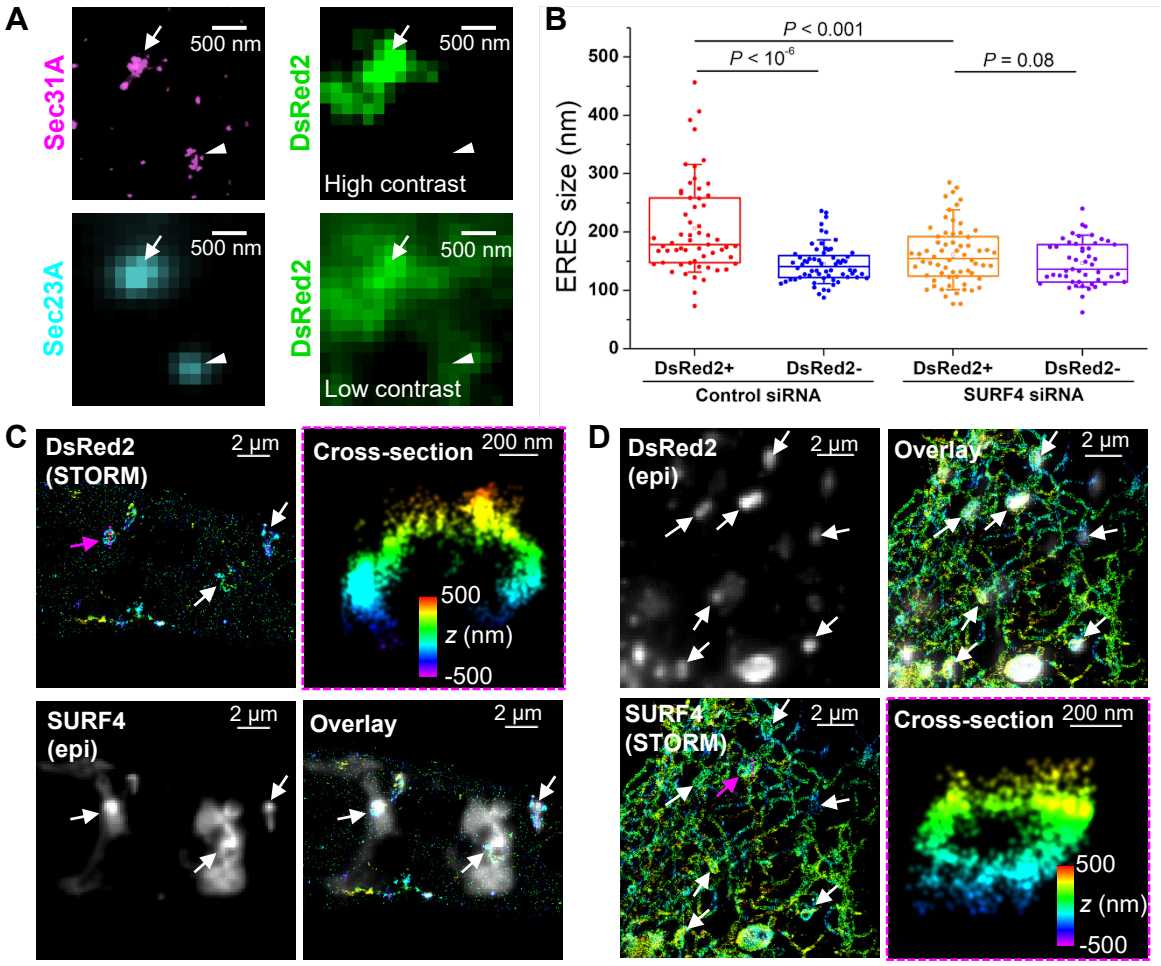

Figure S5. SURF4 and Its Cargo Co-cluster to Expand the ERES, Related to Figure 5

(A) DsRed2-loaded (arrow) and non-loaded (arrowhead) ERESs in a SURF4 siRNA-treated cell. STROM image of Sec31A is shown as magenta, and epifluorescence of EGFP-Sec23A and APV-DsRed2-ER-5 are shown as cyan and green, respectively. With SURF4 knockdown, the APV-DsRed2-ER-5 cargo no longer clustered strongly at the ERES, so that DsRed2-loaded and non-loaded ERESs were subjectively assigned based on enhanced contrast of the epifluorescence image.

(B) Statistics of the sizes of DsRed2-loaded and non-loaded, Sec23A-positive ERESs, based on the STORM-determined sizes of the Sec31A clusters, in control and SURF4 siRNA-treated cells. Whiskers and boxes show 10%, 25%, 50%, 75%, and 90% quantiles. *P* values are calculated by the two-tailed *t* test. n = 4 STORM images were quantified.

(C,D) 3D-STORM of immunolabeled APV-SBP-DsRed2-ER-5 (C) or AcGFP1-SURF4 (D), in comparison with epifluorescence images of AcGFP1-SURF4 (C) or APV-SBP-DsRed2-ER-5 (D) of the same views in a RUSH experiment. For cargo release, 80 µM biotin was added 40 min before sample fixation. Arrows indicate co-clustered large SURF4 and DsRed2 domains. Vertical cross-sections of the STORM images are given for the large co-clusters indicated by the magenta arrows, showing membrane localizations for both proteins. Colors in the 3D-STORM images encode axial positions (depth).

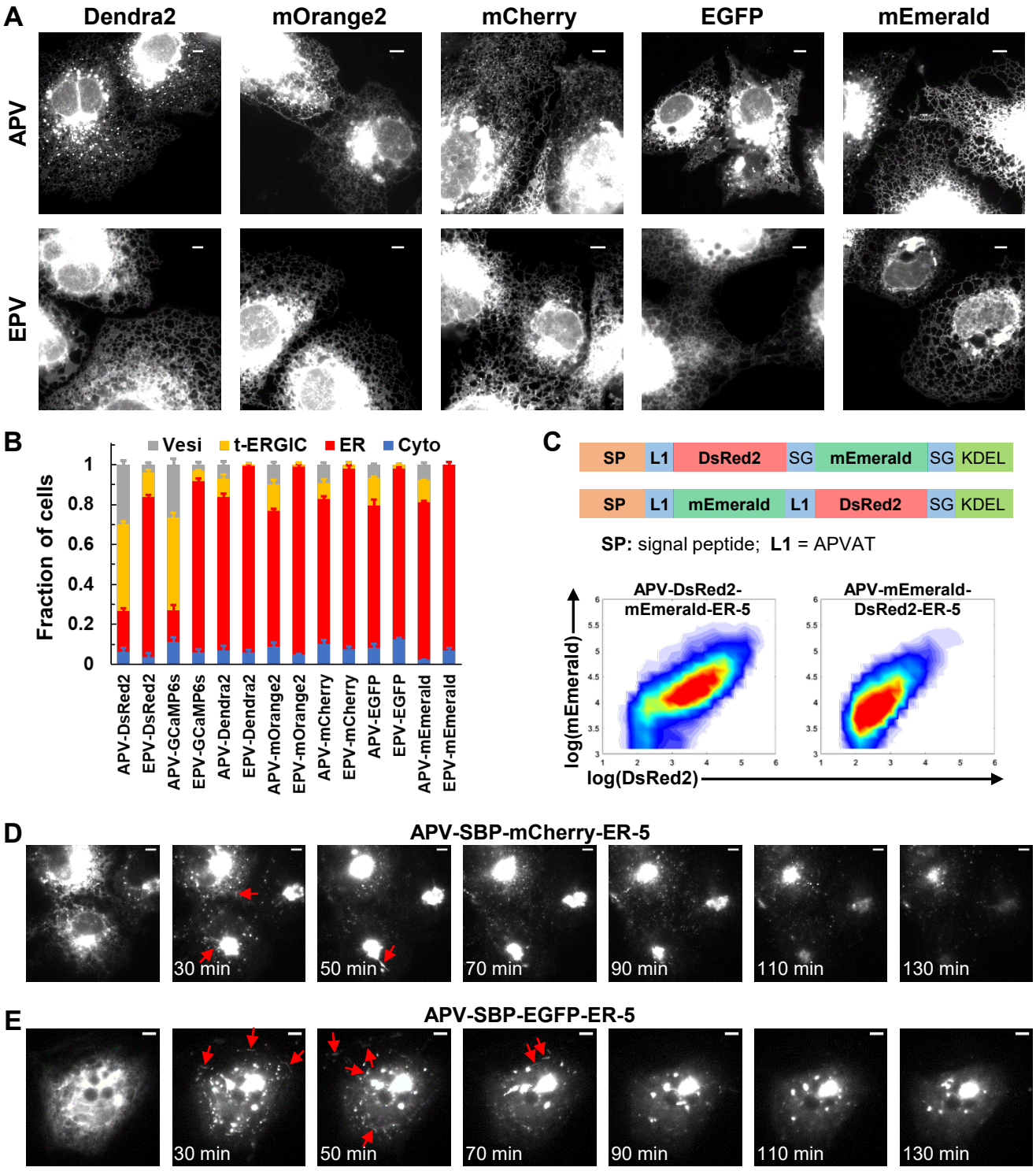

Figure S6. Distinct Steady-State Localizations of Different FP-ER-5 Constructs, Related to Figure 6
(A) Representative fluorescence micrographs of APV/EPV-Dendra2-ER-5, APV/EPV-mOrange2-ER-5, APV/EPV-mCherry-ER-5, APV/EPV-EGFP-ER-5, and APV/EPV-mEmerald-ER-5 in COS-7 cells.
(B) Subcellular distributions of different APV/EPV-FP-ER-5 constructs. The APV-DsRed2 and EPV-DsRed2 data duplicate that of "ER-5" in Figure 1D and that of Figure 3C, respectively. The APV-mOrange2 data duplicates that in Figure 6I. Error bars: SEM (n = 3 with ~50 cells in each replicate).
(C) Sequences and flow cytometry of APV-DsRed2-mEmerald-ER-5 and APV-mEmerald-DsRed2-ER-5.
(D,E) RUSH image sequences of APV-SBP-mCherry-ER-5 (D) and APV-SBP-EGFP-ER-5 (E) showing efficient ER exit and the formation of t-ERGIC. Arrows indicate t-ERGICs.
Scale bars: 5 μm.

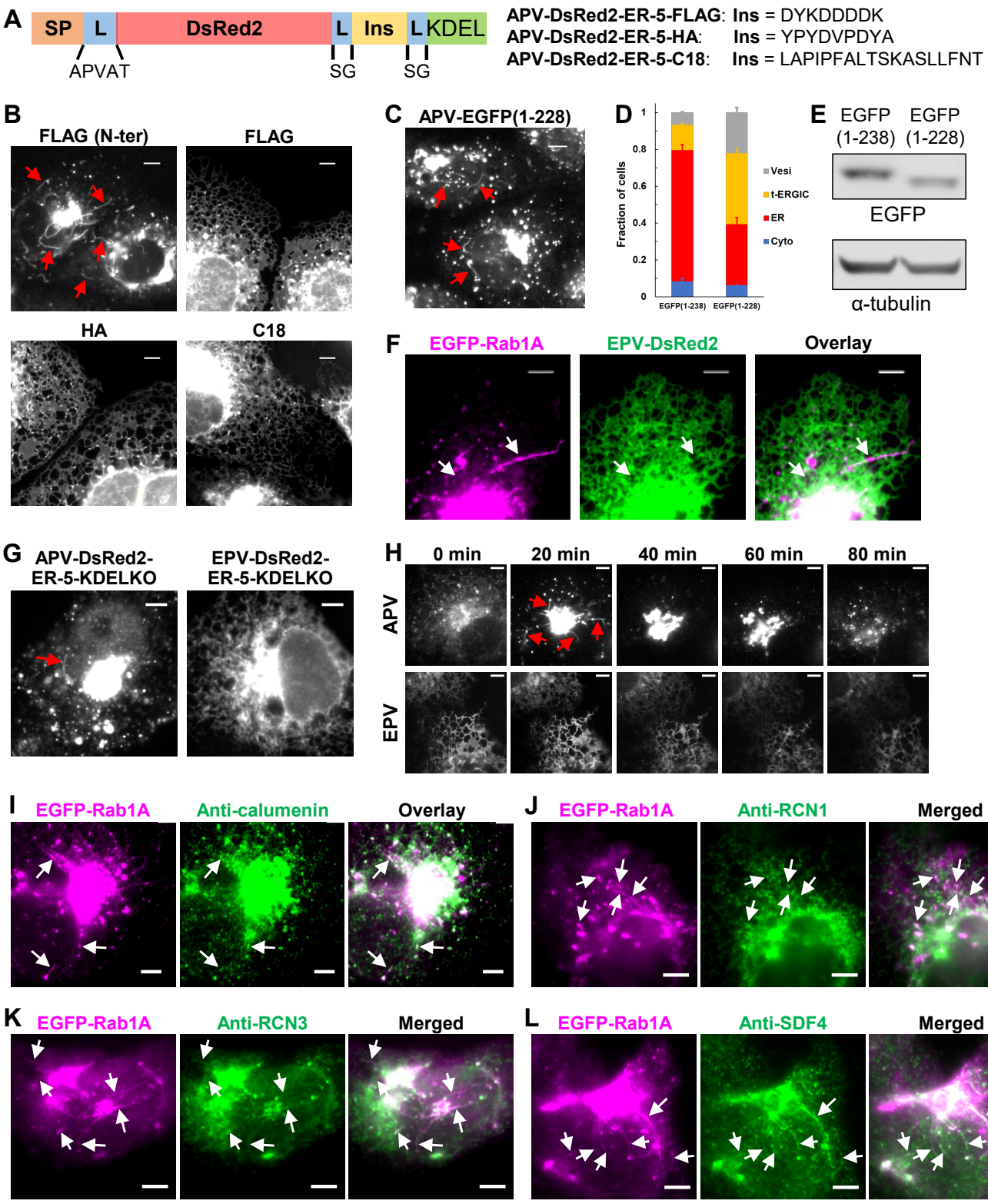

Figure S7. SURF4-KDELR Antagonism Determines the Localization of Cargo Proteins, Related to Figure 6

(A) Schematics of different C-terminal insertions of APV-DsRed2-ER-5.

(B) Representative fluorescence micrographs of APV-FLAG-DsRed2-ER-5, APV-DsRed2-ER-5-FLAG, APV-DsRed2-ER-5-HA, and APV-DsRed2-ER-5-C18 in COS-7 cells.

(C) Representative fluorescence micrograph of APV-EGFP(1-228)-ER-5 in COS-7 cells, showing t-ERGICs.

(D,E) Subcellular distributions (D) and immunoblots (E) of APV-EGFP(1-238)-ER-5 and the C-terminally truncated APV-EGFP(1-228)-ER-5. Error bar: SEM (n = 3 with ~50 cells in each replicate). The APV-EGFP(1-238)-ER-5 subcellular distribution in (D) duplicates "APV-EGFP-ER-5" in Figure S6B.

(F) Two-color live-cell fluorescence micrographs of EGFP-Rab1A and EPV-DsRed2-ER-5-HA in a co-transfected COS-7 cell.
(G) Representative immunofluorescence images of APV/EPV-DsRed2-ER-5-KDELKO in COS-7 cells.
(H) Representative RUSH image sequences of APV/EPV-DsRed2-ER-5-KDELKO in RUSH, showing t-ERGIC-mediated fast ER-to-Golgi transport for the APV (top) but not the EPV (bottom) version. The “20 min” images correspond to Figure 6L.
(I-L) Two-color fluorescence micrographs of EGFP-Rab1A vs. immunolabeled endogenous calumenin (I), RCN1 (J), RCN3 (K), and SDF4 (L) in COS-7 (I) and U2OS (J-L) cells.
Scale bars: 5 μm. Arrows point to t-ERGICs.

SUPPLEMENTAL TABLES

Table S1. Analysis of the P1' N-terminal tripeptide and the C-terminal tetrapeptide for the 61 proteins annotated as "ER-lumen" in a subcellular fractionation-mass spectrometry dataset of HeLa cells (Itzhak et al., 2016), related to Figure 7B.

Lead protein ID	Lead protein name	MS Count	P1' N-term.	SURF4 comp.*	C-term.	KDEL-like&
P14625	Endoplasmin	16455	DDE	0	KDEL	1
P11021	78 kDa glucose-regulated protein	14834	EEE	0	KDEL	1
P27797	Calreticulin	12114	EPA	0	KDEL	1
P07237	Protein disulfide-isomerase	10550	DAP	0	KDEL	1
P13667	Protein disulfide-isomerase A4	8929	EGP	0	KEEL	1
P30101	Protein disulfide-isomerase A3	7193	SDV	0	QEDL	1
Q9Y4L1	Hypoxia up-regulated protein 1	7049	DTL	0	NDEL	1
P50454	Serpin H1	6053	AEV	0	RDEL	1
Q9NYU2	UDP-glucose:glycoprotein glucosyltransferase 1	5755	DSK	0	REEL	1
P14314-2	Glucosidase 2 subunit beta	5273	VEV	0	HDEL	1
Q32P28	Prolyl 3-hydroxylase 1	2550	EVE	0	KDEL	1
Q8IXB1	DnaJ homolog subfamily C member 10	1581	DQD	0	KDEL	1
Q9H488	GDP-fucose protein O-fucosyltransferase 1	1290	WDP	0	RDEF	1
Q14696	LDLR chaperone MESD	1226	AEG	0	REDL	1
Q8NBJ7	Sulfatase-modifying factor 2	1205	QAT	0	PGEL	1
Q6UW63	KDEL motif-containing protein 1	1154	ETG	0	KDEL	1
Q9BT09	Protein canopy homolog 3	521	GAE	0	PDEL	1
Q5NDL2	EGF domain-specific O-linked N-acetylglucosamine transferase	344	GQN	0	HDEL	1
O95994	Anterior gradient protein 2 homolog	258	RDT	0	KTEL	1
Q9Y680-2	Peptidyl-prolyl cis-trans isomerase FKBP7	253	QRQ	0	HDEL	1
Q8IXL7-2	Methionine-R-sulfoxide reductase B3	207	QSG	0	KAEL	1
P23284	Peptidyl-prolyl cis-trans isomerase B	4647	DEK	0	IAKE	0
O00469-2	Procollagen-lysine,2-oxoglutarate 5-dioxygenase 2	3477	ADS	0	FIDP	0
Q02809	Procollagen-lysine,2-oxoglutarate 5-dioxygenase 1	3469	KGD	0	FVDP	0
O60568	Procollagen-lysine,2-oxoglutarate 5-dioxygenase 3	3164	SDR	0	FVDP	0
Q96HE7	ERO1-like protein alpha	1927	EEQ	0	QNIH	0
Q9UBS4	DnaJ homolog subfamily B member 11	1889	GRD	0	LQGY	0
O15460	Prolyl 4-hydroxylase subunit alpha-2	982	EFF	0	TEVD	0
Q15818	Neuronal pentraxin-1	794	QDF	0	RQIN	0
Q92791	Synaptonemal complex protein SC65	425	QYE	0	PELA	0
Q9H173	Nucleotide exchange factor SIL1	357	HQN	0	KELR	0
O95479	GDH/6PGL endoplasmic bifunctional protein	247	QEL	0	AFLG	0
Q9Y2G5	GDP-fucose protein O-fucosyltransferase 2	246	SGQ	0	KITY	0
Q96AY3	Peptidyl-prolyl cis-trans isomerase FKBP10	4278	RGL	0.5	HEEL	1
Q15084	Protein disulfide-isomerase A6	3286	LYS	0.5	KDEL	1
Q8NBS9	Thioredoxin domain-containing protein 5	3266	GRW	0.5	KDEL	1

P30040	Endoplasmic reticulum resident protein 29	2720	LHT	0.5	KEEL	1
Q8NBJ5	Procollagen galactosyltransferase 1	2028	YFP	0.5	RDEL	1
Q14257	Reticulocalbin-2	1894	GKA	0.5	HDEL	1
Q9Y2B0	Protein canopy homolog 2	1857	RRS	0.5	HDEL	1
O95881	Thioredoxin domain-containing protein 12	1356	HNG	0.5	EDEL	1
Q14554	Protein disulfide-isomerase A5	1202	KVS	0.5	KEEL	1
Q9HCN8	Stromal cell-derived factor 2-like protein 1	1111	AKT	0.5	HDEL	1
Q99470	Stromal cell-derived factor 2	779	LGV	0.5	HAEL	1
Q9NYU1	UDP-glucose:glycoprotein glucosyltransferase 2	638	SKS	0.5	HDEL	1
P26885	Peptidyl-prolyl cis-trans isomerase FKBP2	621	TGA	0.5	RTEL	1
Q9H6E4	Coiled-coil domain-containing protein 134	528	TLR	0.5	QSEL	1
Q9UNW1	Multiple inositol polyphosphate phosphatase 1	514	SLL	0.5	SDEL	1
Q6UWW8	Carboxylesterase 3	325	TGP	0.5	QEDL	1
P04844	Dolichyl-diphosphooligosaccharide--protein glycosyltransferase subunit 2	2456	LTP	0.5	RTAH	0
Q14165	Malectin	1824	PGL	0.5	LCRL	0
Q13217	DnaJ homolog subfamily C member 3	1502	GVN	0.5	FHFN	0
P43307	Translocon-associated protein subunit alpha	1008	RGG	0.5	GSDE	0
P43251	Biotinidase	255	AHT	0.5	YERD	0
O60613	15 kDa selenoprotein	254	FGA	0.5	LERI	0
O43852	Calumenin	3514	KPT	1	HDEF	1
Q15293	Reticulocalbin-1	3128	KPT	1	HDEL	1
Q8IVL5	Prolyl 3-hydroxylase 2	1839	GPP	1	KDEL	1
O95302	Peptidyl-prolyl cis-trans isomerase FKBP9	1523	APV	1	HDEL	1
Q96D15	Reticulocalbin-3	1174	KPS	1	HDEL	1
P13674-2	Prolyl 4-hydroxylase subunit alpha-1	2267	HPG	1	SELE	0

* SURF4 compatibility is evaluate based on the P1' N-terminal tripeptide after signal peptide cleavage. 0: containing D, E, or Q. 1: X-P-Y, in which neither X nor Y is D, E, or Q. 0.5: others. Signal peptide cleavage sites were predicted by SignalP5.0 (http://www.cbs.dtu.dk/services/SignalP)

& 1 means a KDEL or KDEL-like C-terminus (Raykhel et al., 2007). 0 means otherwise.